Available online at www.sciencedirect.com

ScienceDirect

Energy Procedia 92 (2016) 42 – 51

Energy Procedia

6th International Conference on Silicon Photovoltaics, SiliconPV 2016

Modelling kinetics of the boron-oxygen defect system

Brett Hallam[a*], Malcolm Abbott[a], Jose Bilbao[a], Phill Hamer[b,a], Nicholas Gorman[a], Moonyong Kim[a], Daniel Chen[a], Katherine Hammerton[a], David Payne[a], Catherine Chan[a], Nitin Nampalli[a], Stuart Wenham[a]

[a]*The University of New South Wales, Sydney, NSW 2052, Australia*
[b]*University of Oxford, Oxford, OX1 2JD, United Kingdom*

Abstract

Here we report on modeling kinetics of the boron-oxygen defect system in crystalline silicon solar cells. The model, as supported by experimental data, highlights the importance of defect formation for mitigating carrier-induced degradation. The inability to rapidly and effectively passivate boron-oxygen defects is primarily due to the unavailability of the defects for passivation, rather than any "weakness" of the passivation reaction. The theoretical long-term stability of modules in the field is investigated as a worst-case scenario using typical meteorological year data and the System Advisor Model (SAM). With effective mounting of the modules, the modelling indicates that even in desert locations, destabilisation of the passivation is no concern within 40 years. We also incorporate the quadratic dependence of the defect formation rate on the total hole concentration, and highlight the influence of changing doping densities or changing illumination intensity on the CID mitigation process.

Peer review by the scientific conference committee of SiliconPV 2016 under responsibility of PSE AG.

Keywords: boron-oxygen; light-induced degradation; carrier-induced degradation; hydrogen passivation; regeneration

1. Introduction

1.1. Boron-oxygen defect system in p-type Czochralski silicon

Crystalline silicon solar cells fabricated on boron-doped Czrochralski (Cz) grown silicon substrates are subject to a degradation of performance when exposed to carrier injection, which for solar cells, is typically induced by exposure to light [1]. This has been attributed to the formation of a boron-oxygen (B-O) complex, although the defect composition is still being heavily debated in the literature [2-7].

Peer review by the scientific conference committee of SiliconPV 2016 under responsibility of PSE AG.
doi:10.1016/j.egypro.2016.07.008

In 2006, Herguth *et al.* presented a method to passivate the boron-oxygen (B-O) defects based on illuminated annealing, hence permanently eliminating the B-O related carrier-induced degradation (CID) [8]. Earlier papers had focused on the temperature range of 50 °C – 230 °C and noted a reduced effectiveness of processes conducted at higher temperatures [8-12]. Similarly to the structure of the defect, significant contradictions have been reported on the mechanisms involved in the permanent passivation process [13-17]. However, strong evidence has shown the involvement of hydrogen [13,16,18-20], and in particular, the importance of hydrogen charge states in the passivation of the defect [14,21-24]. With the advancements in the understanding of the B-O defect and hydrogen passivation mechanisms, recent publications have demonstrated effective passivation of the defects at temperatures of 250 °C – 360 °C using patented hydrogenation processes [22,25-26], and this appears to be the temperature range adopted by tool manufacturers such as Centrotherm [27].

Warranties issued by solar panel manufacturers require that a certain level of performance be maintained for typically 25 years. Based on published reaction rates for the destabilisation reaction [28] and dissociation of the B-O defect [29], the passivated state of the B-O defect is more than 100 times stable than the defect itself for temperatures above 0 °C. However, due to the potential destabilisation of passivated B-O defects in the field, questions over long-term stability of the passivation are often raised.

1.2. Modelling the boron-oxygen defect system

Previous studies modelling the kinetics of the B-O defect system have investigated a variety of potential influences on the system. Those studies have typically used three-state models to describe the defect system, with simple reaction rates consisting of an attempt frequency and an activation energy [11, 30-33]. In those studies, no explicit influence of either the doping concentration or carrier concentrations were included. In another study, reaction rates involved normalised concentrations of substitutional boron, interstitial oxygen dimers and a mystery compound, X, that is now presumed to be hydrogen [9]. Again, in that study no dependence was included for the influence of carrier-injection. Gläser *et al.* included occupational probability of hydrogen charge states to participate in the defect passivation reaction [24]. However, the fractional concentrations of hydrogen charge states were assumed constant for a given illumination intensity, and hence no dependence on variations in the hydrogen charge state concentrations were considered throughout the process as the carrier lifetime evolves through the degradation-passivation cycle [24].

Studies exploring methods to accelerate the passivation of the defect have suggested that the speed of B-O defect passivation is primarily dependent on the time-constant for the passivation reaction [10]. However, that assumption did not include the influence of the availability of defects for passivation. In that study, time constants given for the destabilisation reaction were given at temperatures of 25 °C and 60 °C. It was concluded that the reported values of >8,800 years and >53 years, respectively, were sufficiently long that destabilisation would not be a major problem in the lifespan of a typical solar cell [10]. This was in agreement with earlier predictions by Herguth *et al.* [30], which also noted that any increased cell operating temperature would most likely be accompanied by illumination that could enable the passivation reaction to counteract the destabilisation reaction. However, operating temperatures of modules are highly variable, and in certain instances modules can operate well in excess of 60 °C.

Here we use a three-state model to describe the B-O defect system and perform a worst-case scenario numerical simulation of photovoltaic (PV) modules in operation to study the potential destabilisation of the B-O defect passivation. This is based on experimentally obtained values for the destabilisation reaction [28], predicted module temperatures using the System Advisor Model (SAM) (version 2015.06.30) from the National Renewable Energy Laboratory (NREL) [34-35] from typical meteorological year data. The study was extended to investigate the potential of passivating B-O defects in the field using the same principle.

We also discuss the model in terms of the rate-limiting reactions for the passivation of B-O defects. Our results show that in contrast to previous claims that the hydrogenation rate limits the speed at which defects can be passivated, with recently reported values of the passivation reaction rate, the speed at which defects are passivated is limited by the availability of defects for passivation, and therefore, the defect formation rate.

Further modifications are made to the model to reflect the enhanced understanding for the behaviour of the B-O defect, with the ability to accelerate the defect formation rate in p-type silicon by using high intensity illumination to increase the total hole concentration [36]. These include the quadratic dependence of the defect formation rate on the

total hole concentration as demonstrated in both n-type [37] and p-type silicon [38]. Therefore, the model includes the dependence on boron doping concentration, illumination intensity, injection-level-dependent minority carrier lifetime and the time-varying minority/majority carrier concentrations on the defect formation rate.

2. Basic three-state mathematical model for the boron-oxygen defect system

Simulations in this paper are performed using a kinetic three-state model previously used in [11, 30, 33]. In this model, the three states are as follows:

- A – recombination inactive state before defect formation
- B – recombination active state after defect formation
- C – recombination inactive and stable state after hydrogen passivation

Moving from state A to state B typically occurs at low temperatures (below 50 °C) under illumination, or more precisely, with carrier injection. Moving from state B to state C also requires illumination (or carriers), however this is typically performed at higher temperatures of 50 °C – 360 °C [8-12, 22, 25-26]. Moving back from the stable state C to state B as well as from state B to state A occurs at elevated temperatures (typically in the dark), or with insufficient illumination to allow the more desirable transitions to dominate. Fig. 1 shows a diagrammatic representation of the three-state system and relevant reactions.

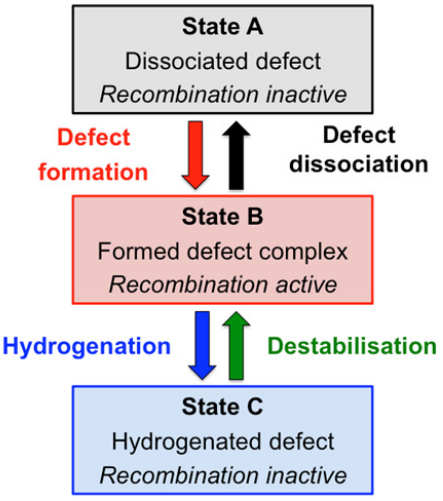

Fig. 1. Diagrammatic representation for the three-state B-O defect system associated with CID in boron-doped Cz silicon.

The associated mathematical equations describing the system of differential equations are shown in Equations 1-3 below, where N_i is the population in state i (for i=A,B,C), and k_{ij} is the reaction rate for the transition from state i to state j, (i,j = A,B,C, but $i \neq j$). Equation 4 shows the reaction rate k_{ij}, in terms of the attempt frequency (ν_{ij}) and corresponding activation energy (Ea_{ij}), where k_b is the Boltzmann constant and T is the temperature in Kelvin. The activation energies and attempt frequencies are shown in Table 1. In this model, no direct transitions between state A and C occurs (i.e. $k_{AC} = k_{CA} = 0$). This is discussed in detail in reference [33].

$$\frac{\partial N_A}{\partial t} = k_{BA} \cdot N_B - k_{AB} \cdot N_A \quad (1)$$

$$\frac{\partial N_B}{\partial t} = k_{AB} \cdot N_A + k_{CB} \cdot N_C - (k_{BA} + k_{BC}) \cdot N_B \quad (2)$$

$$\frac{\partial N_C}{\partial t} = k_{BC} \cdot N_B - k_{CB} \cdot N_C \quad (3)$$

$$k_{ij} = \nu_{ij} \cdot e^{\left(\frac{-Ea_{ij}}{k_b T}\right)} \quad (4)$$

Table 1. Activation energies (Ea_{ij}) and characteristic frequencies (v_{ij}) for different state transitions (T_{ij}) from state i to state j in the B-O defect system. The characteristic frequency for defect formation assumes an effective dopant concentration of N_A=1x10^{16} /cm^3 under low injection conditions, and the characteristic frequency for defect passivation is under 2.7 suns illumination.

Mechanism	Attempt frequency (v)	Activation energy (E_a)	Reference
Defect formation (T_{AB})	4x10^3 /s	0.475 eV	[29]
Defect dissociation (T_{BA})	1x10^{13} /s	1.32 eV	[29]
Defect passivation (T_{BC})	1.25x10^{10} /s	0.98 eV	[28]
Destabilisation (T_{CB})	1x10^9 /s	1.25 eV	[28]

3. Modelling the long-term behavior of boron-oxygen defects with typical meteorological year data

With the reactions in the B-O defect system being temperature dependent, it is important to understand the operating temperatures of modules in the field in order to assess the long-term stability of CID mitigation in modules. Whilst the actual operating temperature of modules in the field requires complex modelling, and is dependent on a large number of variables, two key parameters that influence the operating temperature are the ambient temperature and solar insolation. Both of these differ substantially across the globe and throughout the year.

Simulations in this work used typical meteorological data in hour intervals for an entire year from Hamburg (Germany), Sydney (Australia), Tucson (United States of America) and Wuhan (China). The PV system investigated was a rack-mounted system installed on a roof tilted at 15° towards the equator. A 100 mm air-gap was assumed between the roof and the module, to represent a typical residential PV system. Therefore, the system has partial ventilation at the rear of the module to assist with cooling. Simulations for the output power, efficiency and temperature of the modules in operation were obtained using the SAM (version 2015.06.30) [34-35]. Figure 2(a) shows a sample distribution of the module operating temperatures experienced in Tucson. As shown, maximum operating temperatures for the module throughout the year were in excess of 90 °C. Figure 2(b) shows the correlation between the solar insolation in the plane of array (POA) and operating temperature of the module. The solar insolation strongly affects the operating temperature of the module, however with a large spread of the data, other influences such as the ambient temperature and wind speed are likely to have a strong influence.

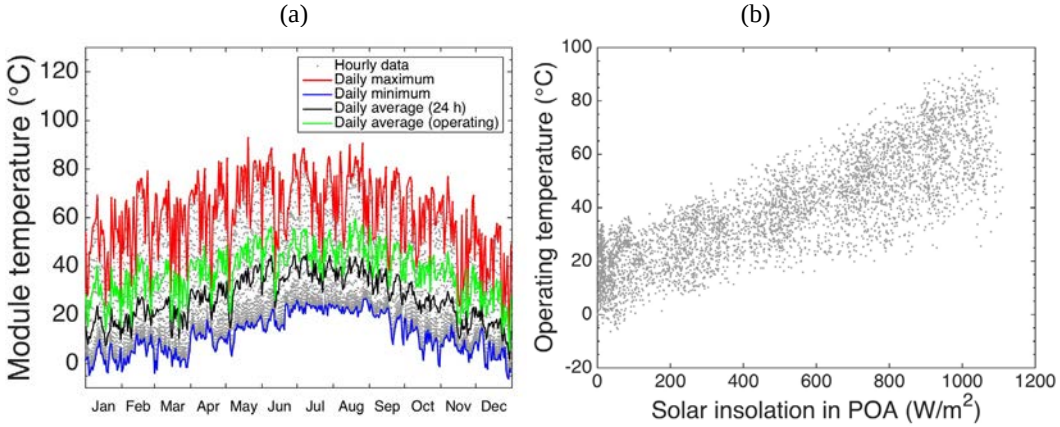

Fig. 2. (a) Hourly module temperature on a rack-mounted system installed in Tucson showing the daily minimum and maximum temperatures of the module. The average daily temperature during operating hours, and as a 24-hour average are also shown. (b) Correlation between the solar insolation in plane of array (POA) and the operating temperature of the module in Tucson.

A substantial variation in the ambient temperature and operating temperature for all locations were experienced throughout the year. Figure 3(a) shows the frequency distribution of the ambient temperature for each location in terms of the number of hours per year at a given temperature (in 1 °C bins). Hamburg experiences the lowest average ambient temperatures whilst Tucson experiences the highest temperatures. Figure 3(b) shows the corresponding frequency distribution for the module operating temperatures. Similarly, Hamburg has the lowest module operating temperatures, rarely in excess of 60 °C (47 hours/year), whilst Sydney (298 hours/year), Tucson (755 hours/year) and Wuhan (441 hours/year) experience operating temperatures in excess of 60 °C, and can experience temperatures in excess of 80 °C. For Tucson, module operating temperatures in excess of 80 °C are reached for 90 hours/year.

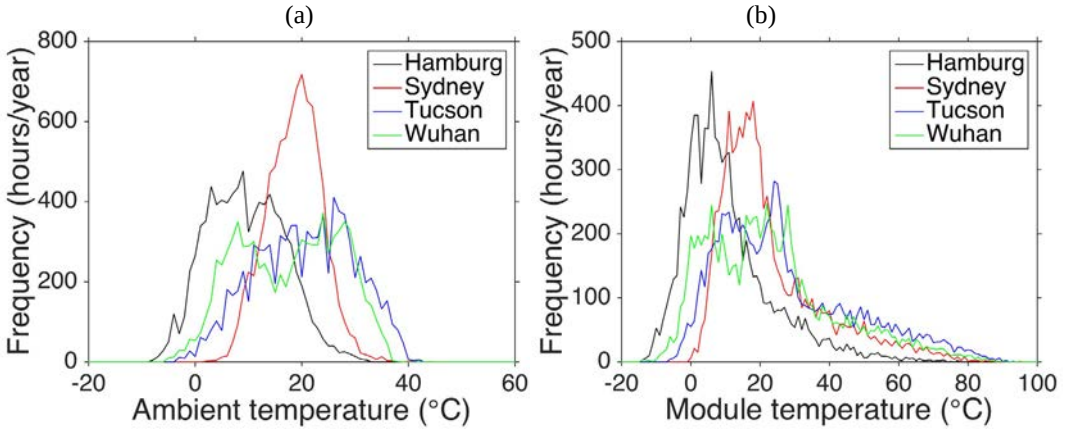

Fig. 3. Frequency distribution (binned in 1 °C increments) for (a) ambient temperatures and (b) module operating temperatures.

3.1. Modelling long-term destabilisation of the B-O defect with typical meteorological year data

The time-dependent module operating temperatures were applied to the three-state model to assess the long-term stability of passivated B-O defects over a 40-year period. For this, the 1-year data output of module operating temperatures from the SAM was repeated 40 times. As a worst-case scenario, the passivation reaction was disabled, i.e. no re-passivation occurs for any passivated defects that are destabilised. However, it should be noted that in reality, any condition that causes a destabilisation of the passivated defects is likely to also enable the passivation reaction. Figure 4 shows the fraction of defects that are passivated as a function of time, starting from the case where 100% of defects were passivated (i.e. N_C=1). This corresponds to a case where the advanced hydrogenation process was incorporated during the manufacture of the solar cells/module. As shown, the amount of potential destabilisation is heavily dependent on the location.

Modules installed in Hamburg showed no significant predicted destabilisation of the defects (less than 2% of defects). Due to the higher module operating temperatures in other locations, up to 30% of passivated defects could destabilise over a 40-year period. The worst location of those studied is Tucson due to the highest average temperatures, and hence increased time-averaged reaction rate for the destabilisation reaction. This destabilisation of 30% of defects was then translated into an efficiency loss of the modules. Here we assumed a 0.85% absolute efficiency loss due to CID if all defects were active. Therefore, the 30% destabilisation would result in an efficiency drop of approximately 0.35% absolute. In contrast, modules in Hamburg would lose less than 0.03% absolute.

Then, we include a potential passivation reaction to counteract destabilisation, as would occur during real operation. Here we assume an attempt frequency for defect passivation that is linearly proportional to the solar insolation in POA, with a value of ν_{BC}=4.6x10^9 /s per sun, consistent with reference [28] and Al-BSF cells fabricated at UNSW. To reduce the effective destabilisation of the defects and have an efficiency loss over the 40-year period in Tucson of less than 0.05% absolute, an ongoing hydrogenation reaction rate of (1.38x10^7 /s per sun) would be required. This is 0.3% of the value observed experimentally in open circuit at 1-sun. Therefore, it would not appear that any long-term destabilisation is a concern for modules in the field. This is also consistent with

observations by Lee *et al.*, who observed a gradual recovery of the modules operating out in the field at maximum power point at 50 °C [39]. In that work, 40% of the open circuit voltage (V_{OC}) could be recovered within 600 hours. This corresponds to a hydrogenation reaction of approximately 10% of that in open circuit at 1-sun. Extended simulations using that reaction rate would suggest that full recovery should be achieved in approximately 8 months. However it is unclear whether the recovery of the V_{OC} in that paper had saturated after 600 hours [39].

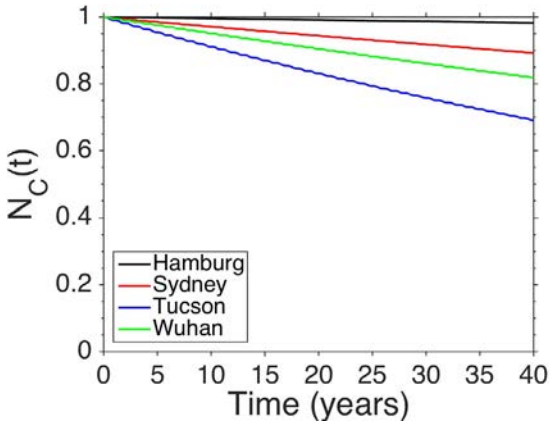

Fig. 4. Potential destabilisation of B-O defects over a 40-year period assuming no re-passivation of destabilised defects. N_C represents the fraction of defects in the passivated state.

4. Importance of the availability of defects for passivation

Previous studies have suggested that with time constants of less than 2 s for the passivation reaction, effective (99%) CID mitigation can be realised in 10 s [10]. However, that assumption requires that at all times all defects are available for passivation. Unfortunately that is not the case for the B-O defect system. Defects require formation prior to passivation, and a thermal dissociation of the defects can occur. Both of these effects reduce the availability of the defects for passivation [33]. Fig. 5(a) shows a mathematical simulation for two different cases of a 230 °C CID mitigation process. In Case 1, the influence of the availability of defects for passivation is ignored ($N_B(0)=1$ and $\nu_{BA}=0$). Hence in Case 1, defects are always available for passivation and it takes 2.5 s to passivate 99% of the defects. Case 2 includes the influence of defect availability for passivation, i.e. defects require formation before passivation ($N_A(0)=1$), and defect dissociation can occur. In Case 2, defects are NOT always available for passivation. This is an accurate representation of solar cells directly after metallisation firing. In Case 2, it takes 115 s to passivate 99% of defects. Fig. 5(b) shows a theoretical simulation of the effectiveness of CID mitigation (i.e. the percentage of defects in the permanently passivated state), as a function of processing temperature for the same two cases. In Case 1, 99% of B-O defects should passivated (in state C) when using a 500°C CID mitigation process. This curve is in agreement with a recently presented method for determining the maximum temperature for effective B-O passivation [11]. However that method (and the dashed blue curve) are not consistent with experimental data published in the literature (also shown in Fig. 1(b)) [10]. This data shows a decreasing effectiveness of the CID mitigation for temperatures beyond 230°C. The data is consistent with Case 2, where the influence of defect availability is included. Therefore, the speed at which defects can be passivated and hence CID in p-type silicon can be mitigated is heavily dependent on the availability of defects for passivation. To accelerate the mitigation process, defect formation should be accelerated, such as by using high intensity illumination.

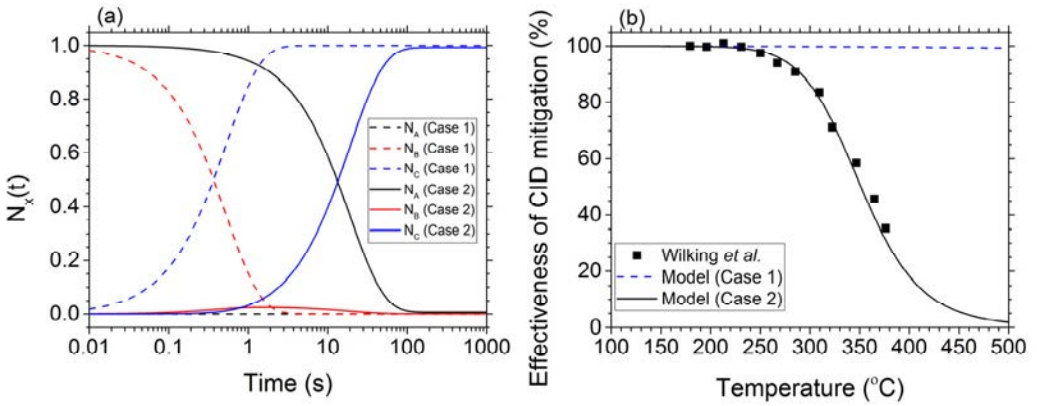

Fig. 5. Theoretical simulations for a CID mitigation process (a) performed at 230°C and showing the defect state population fractions ($N_x(t)$), and (b) the effectiveness of CID mitigation (equivalent to N_C given a sufficient time to reach steady state). Case 1 (dashed curves) ignores the influence of defect availability. Case 2 (solid curves) includes the influence of defect availability. Data in (b) sourced from reference [28].

5. Incorporating the hole-dependent defect formation rate into the kinetic model

In light of recent demonstrations of accelerated defect formation using high intensity illumination [36], further developments of the model are required. In this section, we include the quadratic dependence of the reaction rate for defect formation on the total hole concentration [37-38]. Hence two additional states are included in the ordinary differential equation (ODE) solver to monitor the excess electron and excess hole concentrations. Here, the defect formation rate used is shown in Equation 5 below, where C=4.55x10^{-30} cm^6/s and p is the total hole concentration. An activation energy of 0.415 eV was used in accordance with Hamer *et al.* from this conference [38].

$$v_{AB} = C \cdot p^2, \tag{5}$$

The time-dependent lifetime of the silicon is monitored in the model, taking into account Auger recombination (assuming the Richter model) [40], Schockley-Read-Hall (SRH) recombination, a hypothetical injection-level-independent bulk lifetime component ($\tau_{bulk,0}$) and a total dark saturation current density (J_0), the thickness and doping concentration of the material. The model includes the ability to specify the generation rate of electron-hole pairs through an illumination intensity, with the assumption that a 1-sun process is equivalent to a generation rate of 2.5x10^{17} electron-hole pairs/cm^2/s. For SRH recombination, a fixed ratio of the electron lifetime to the hole lifetime ($\tau_{SRH,p}$ / $\tau_{SRH,n}$) of 20 is assumed (consistent with modelling performed on lifetime test samples in our previous work), with an energy level of 0.41 eV below the conduction band [41]. The SRH lifetime components are modulated throughout the process based on the $\tau_{SRH,p}$ and $\tau_{SRH,n}$ values of the sample in the fully degraded state ($\tau_{SRH,n}(N_B=1)$ and $\tau_{SRH,p}(N_B=1)$). Here an inverse proportionality is assumed, i.e. if only 50% of defects are formed, then the SRH lifetime components are double that of the corresponding values in the fully degraded state. All lifetimes and carrier concentrations are based on room-temperature measurements and the reaction rates for hydrogenation are assumed to be constant.

One method to increase the availability of defects for passivation by accelerating defect formation is to increase the equilibrium hole concentration. Here we assume a 1-sun process on modest lifetime material ($\tau_{bulk,0}$=200 µs, J_0=300 fA/cm^2, $\tau_{SRH,n}(N_B=1)$= 40 µs and $\tau_{SRH,p}(N_B=1)$= 800 µs) and vary the bulk doping concentration of the material. It should be noted that modulating the doping concentration, also modulates the injection-level-dependent recombination activity of the defect, even assuming the same defect concentration and electron/hole SRH lifetime components. Figure 6 shows the fraction of passivated defects as a function of time ($N_C(t)$) for a range of effective doping densities ranging from lightly boron-doped silicon wafers (N_a=1x10^{15} /cm^3) to heavily boron-doped silicon wafers (N_a=1x10^{17} /cm^3). The figure shows that increasing the boron-doping concentration can (a) increase the effectiveness of the passivation, and (b) result in a more rapid passivation of the defects. Hence, even though SRH

recombination due to the boron-oxygen defect could be more severe for more heavily doped silicon, the use of heavily doped silicon will assist with the mitigation of CID.

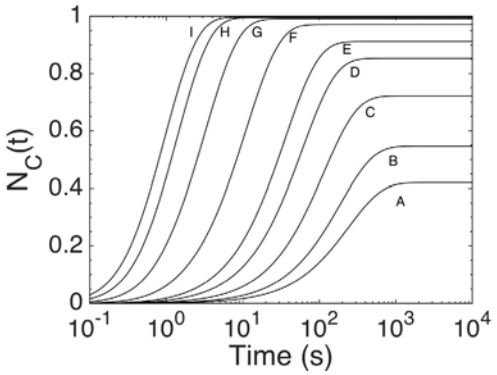

Fig. 6. Theoretical simulations of the fraction of passivated defects as a function of time for a 1-sun process performed at 250°C highlighting the influence of boron-doping density on accelerating the mitigation of CID. Letters in the graph correspond to the boron-doping density (N_a) in /cm^3, and are as follows: A=1x10^{15}, B=2x10^{15}, C=4x10^{15}, D=7x10^{15}, E=1x10^{16}, F=2x10^{16}, G=4x10^{16}, H=7x10^{16}, I=1x10^{17}.

Another method to increase the availability of defects for passivation is to increase the illumination intensity, to drive the silicon into high-injection [36]. Here we assume the same lifetime parameters as above, with a boron-doping concentration of N_a=1x10^{16} /cm^3 while varying the illumination intensity from 0.1 suns up to 100 suns. Figure 7(a) shows the operating point (Δp) of the process for a given illumination intensity, and the corresponding total hole concentration (p). To have any substantial increase in the total hole concentration, an illumination intensity in excess of 1 sun is required. It should be noted that in this image, samples are assumed to be in the dark annealed state. Figure 7(b) shows the influence of the increased total hole concentration on accelerating the mitigation of CID for selected illumination intensities. As shown, increasing the illumination from 1 sun to 100 suns can accelerate the mitigation of CID by approximately 1 order of magnitude. Here, the time-varying injection level of the operating point was taken into account. Note that the hydrogenation reaction rate is assumed to be independent of illumination intensity in this section. This is consistent with Hamer *et al.* who observed that the hydrogenation reaction was not significantly increased by using high-intensity illumination [26]. The same could be achieved by increasing the minority carrier lifetime of the silicon. This is clearly advantageous for solar cells, due to the enhancements in efficiency (not shown). However, for CID mitigation processes, this also acts to accelerate defect formation though an increase in the majority carrier concentration throughout the process.

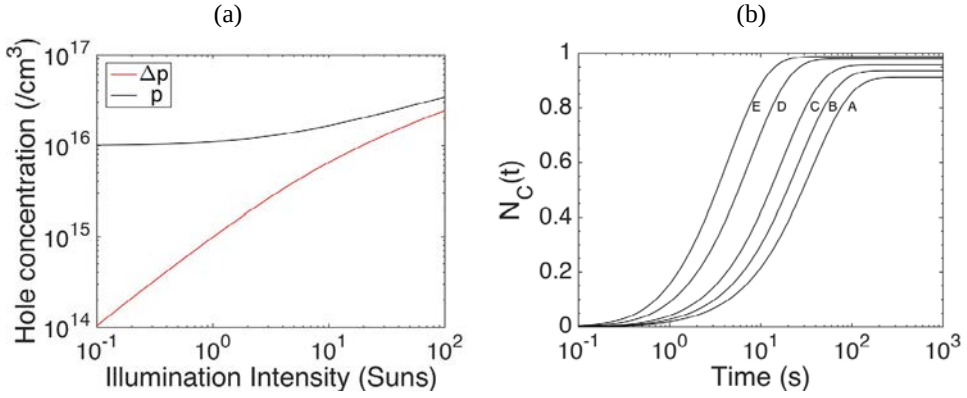

Fig. 7. (a) Excess hole concentration and total hole concentration for the operating point of CID mitigation processes at 250°C for various illumination intensities (assuming the dark annealed state). (b) Theoretical simulations of CID mitigation process. A=1 sun, E=4 suns, C = 10 suns, D=40 suns, E=100 suns.

6. Conclusions

In this paper we used kinetic models to study the behavior of the B-O defect system. Long-term simulations were performed on modules in the field to simulate a potential destabilisation of passivation. The extent of destabilisation (ignoring any on-going re-passivation of defects), was heavily dependent on the location, due to differences in temperature. Over a 40-year period, a destabilisation of defects in Hamburg was of no concern, whilst in warmer locations such as Tucson, up to 30% of defects could destabilise, which would result in an efficiency drop of 0.35% absolute given the assumptions used in this paper. To counteract this efficiency drop, a relatively low passivation rate of 0.3% of that for passivation processes performed at 1-sun in open circuit would be required. Based on experimental data published in literature [39], modules can easily achieve the required hydrogenation reaction rates under conditions similar to operation in the field. Therefore, any ongoing destabilisation of passivated B-O defects does not appear to be an issue for the long-term stability of photovoltaic modules.

The availability of defects was also shown to have a large impact on the time to passivate defects, and the effectiveness of passivation at elevated temperatures. It appears that this is a key factor in limiting the possible temperatures that can be used for effective CID mitigation.

The quadratic dependence of the defect formation rate on the total concentration of holes was incorporated into the model. This could therefore take into account variations in the reaction rate for defect formation on the boron doping concentration, illumination intensity, and the time and injection-level-dependent minority carrier lifetime. Therefore, the model could include the impact of time-varying minority/majority carrier concentrations through the defect formation/passivation cycle. Two key methods to accelerate the mitigation of CID were modelled; (1) increasing the boron-doping concentration, and (2) increasing the illumination intensity. Other options of increasing the minority carrier lifetime were also discussed.

Acknowledgements

This Program has been supported by the Australian Government through the Australian Renewable Energy Agency (ARENA) and the Australian Centre for Advanced Photovoltaics (ACAP). The views expressed herein are not necessarily the views of the Australian Government, and the Australian Government does not accept responsibility for any information or advice contained herein. The authors would also like to thank the commercial partners of the ARENA 1-060 advanced hydrogenation project, and the UK Institution of Engineering and Technology (IET) for their funding support for this work through the A.F. Harvey Engineering Prize.

References

[1] Fischer H, Pschunder W. Investigation of photon and thermal induced changes in silicon solar cells. Proc. 10th IEEE PVSC 1973;404.
[2] Schmidt J, Bothe K. Structure and transformation of the metastable boron- and oxygen-related defect center in crystalline silicon. Physics Review B 2004;69:024107.
[3] Bourgoin J, de Angelis N, Strobl G. Light Induced Degradation of Si Cells. Model of a Metastable Defect. Proc. 16th EU PVSEC 2000;1356.
[4] Voronkov V, Falster R. Latent complexes of interstitial boron and oxygen dimers as a reason for degradation of silicon-based solar cells. Journal of Applied Physics 2010;107(5):053509.
[5] Voronkov V, Falster R, Batunina A. Modelling lifetime degradation in boron-doped Czochralski silicon. physica status solidi (a) 2011;208(3):576-579.
[6] Voronkov V, Falster R, Lim B, Schmidt J. Permanent recovery of electron lifetime in pre-annealed silicon samples: A model based on Ostwald ripening. J. App. Phys. 2012;112(11):113717.
[7] Möller C, Lauer K. Light-induced degradation in indium-doped silicon. physica status solidi (RRL)-Rapid Research Letters 2013;7(7):461-464.
[8] Herguth A, Schubert G, Käs M, Hahn G. A new approach to prevent the negative impact of the metastable defect in boron doped Cz silicon solar cells. Proc. 4th IEEE WCPEC 2006; p. 940-943.
[9] Lim B, Hermann S, Bothe L, Schmidt J, Brendel R. Permanent deactivation of the boron-oxygen recombination center in silicon solar cells. Proc. 23rd European PVSEC 2008;1018-1022.
[10] Wilking S, Engelhardt J, Ebert S, Beckh C, Herguth, Hahn G. High Speed Regeneration of BO-Defects: Improving Long-Term Solar Cell Performance within Seconds. Proc. 29th European PVSEC 2014;366-372.
[11] Wilking S, Forster M, Herguth A, Hahn G. From simulation to experiment: Understanding BO-regeneration kinetics. Solar Energy Mat. and Solar Cells 2015;142:87-91.

[12] Herguth A, Schubert G, Käs M, Hahn G, Melnyk I. Method for fabricating a photovoltaic element with stabilised efficiency, US Patent 8,263,176;2012.
[13] Münzer, K. Hydrogenated Silicon Nitride for Regeneration of Light Induced Degradation. Proc. 24th European PVSEC 2009;1558-1561.
[14] Hallam B, Hamer P, Wenham S, Abbott M, Sugianto A, Wenham A, Chan C, Xu Q, Kraiem J, Degoulange J, Einhaus R. Advanced Bulk Defect Passivation for Silicon Solar Cells. IEEE Journal of Photovoltaics. 2014;4(1):88–95.
[15] Walter D, Lim B, Bothe K, Voronkov V, Falster R, Schmidt J. Effect of rapid thermal annealing on recombination centres in boron-doped Czochralski-grown silicon. Applied Physics Letters. 2014;104(4):042111.
[16] Nampalli N, Hallam B, Chan C, Abbott M, Wenham S. Evidence for the role of hydrogen in the stabilization of minority carrier lifetime in boron-doped Czochralski silicon. Applied Physics Letters 2015;107(17):173501.
[17] Mchedlidze T, Weber J. Direct detection of carrier traps in Si solar cells after light-induced degradation. physica status solidi (RRL)-Rapid Research Letters 2015;9(2):108-110.
[18] Krugel G, Wolke W, Geilker J, Rein S, Preu R. Impact of Hydrogen Concentration on the Regeneration of Light Induced Degradation. Energy Procedia. 2011;8:47–51.
[19] Dubois S, Tanay F, Veirman J, Enjalbert N, Stendera J, Butté S, . The BOLID Project: Suppression of the Boron-Oxygen Related Light-Induced-Degradation. Proc. 27th European PVSEC, Frankfurt, Germany. 2012;749–754.
[20] Wilking S, Herguth A, Hahn G. Influence of hydrogen on the regeneration of boron-oxygen related defects in crystalline silicon. Journal of Applied Physics 2013;113(19):194503.
[21] Hallam B, Wenham S, Hamer P, Abbott M, Sugianto A, Chan C, Wenham A, Eadie M, Xu, G. Hydrogen passivation of B-O defects in Czochralski silicon. Energy Procedia. 2013;38:561–570.
[22] Wenham S, Hamer P, Hallam B, Sugianto A, Chan C, Song L, Lu PH, Wenham AM, Mai L, Chong CM, and Xu GX, and Edwards MB. Advanced hydrogenation of silicon solar cells. US Patent 9,190,556;2015.
[23] Sun C, Rougieux F, Macdonald D. A unified approach to modelling the charge state of monatomic hydrogen and other defects in crystalline silicon. Journal of Applied Physics 2015;117(4):045702.
[24] Gläser M, Lausch D. Towards a Quantitative Model for BO Regeneration by Means of Charge State Control of Hydrogen. Energy Procedia 2015;77:592-598.
[25] Hallam B. Hamer P, Wang S, Song L, Nampalli N, Abbott M, Chan C, Lu D, Wenham A, Mai L, Borojevic N, Li A, Chen D, Kim M, Azmi A, Wenham S. Advanced Hydrogenation of Dislocation Clusters and Boron-oxygen Defects in Silicon Solar Cells. Energy Procedia 2015;77:799-809.
[26] Hamer P, Hallam B, Abbott M, Chan C, Nampalli N, Wenham S. Investigations on accelerated processes for the boron-oxygen defect in p-type Czochralski silicon. Solar Energy Materials and Solar Cells 2016;145:440-446.
[27] Pernau T, Romer O, Scheiffele W, Reichart A, Jooß W. Rather High Speed Regeneration of BO-Defects: Regeneration Experiments with Large Cell Batches31st European PVSEC 2015;918.
[28] Wilking S, Beckh C, Ebert S, Herguth A, Hahn G. Influence of bound hydrogen states on BO-regeneration kinetics and consequences for high-speed regeneration processes. Solar Energy Materials and Solar Cells 2014;131:2–8.
[29] Bothe K, Schmidt J. Electronically activated boron-oxygen-related recombination centers in crystalline silicon. Journal of Applied Physics 2006;99(1):013701.
[30] Herguth A, Hahn G. Kinetics of the boron-oxygen related defect in theory and experiment. J. of Applied Physics. 2010;108(11):114509.
[31] Hallam B, Abbott M, Nampalli N, Hamer P, Wenham S. Implications of Accelerated Recombination-Active Defect Complex Formation for Mitigating Carrier-Induced Degradation in Silicon. IEEE Journal of Photovoltaics 2015;6:92-99.
[32] Hahn G, Wilking S, Herguth A. BO-Related Defects: Overcoming Bulk Lifetime Degradation in Crystalline Si by Regeneration. Solid State Phenomena 2015;242:80-89.
[33] Hallam B, Abbott M, Nampalli N, Hamer P, Wenham S. Influence of the Formation- and Passivation Rate of Boron-Oxygen Defects for Mitigating Carrier-Induced Degradation in Silicon Within a Hydrogen-Based Model. Journal of Applied Physics 2016;119:065701.
[34] de Soto W, Klein S, Beckman W. Improvement and validation of a model for photovoltaic array performance. Solar energy 2006;80(1):78-88.
[35] Neises T. Development and validation of a model to predict the cell temperature of a photovoltaic cell. MS Thesis, University of Wisconsin-Madison, 2011.
[36] Hamer P, Hallam B, Abbott M, Wenham S. Accelerated formation of the boron-oxygen complex in p-type Czochralski silicon. physica status solidi (RRL) 2015;9(5):297-300.
[37] Schön J, Niewelt T, Broisch J, Warta W, Schubert M. Characterization and modelling of the boron-oxygen defect activation in compensated n-type silicon. Journal of Applied Physics 2015;118:245702.
[38] Hamer P, Nampalli N, Hameiri Z, Kim M, Chen D, Gorman N, Hallam B, Abbott M, Wenham S. Boron-Oxygen Defect Formation Rates and Activity at Elevated Temperatures, *This conference* (6th International Conference on Silicon PV) 2016.
[39] Lee K, Kim M, Lim J, Ahn J, Hwang M, Cho E. Natural Recovery from LID: Regeneration under Field Conditions?. Proc. 31st European PVSEC 2015;1837.
[40] Richter A, Werner F, Cuevas A, Schmidt J, Glunz S. Improved parameterization of auger recombination in silicon. Energy Procedia 2012;27:88-94.
[41] Rein S, Diez S, Falster R, Glunz S. Quantitative correlation of the metastable defect in Cz-silicon with different impurities. Proc. 3rd World Conference on Photovoltaic Energy Conversion 2003;2:1048-1052.